Published by Institute of Physics Publishing for SISSA
Received: *January 4, 2005*
Accepted: *May 2, 2005*
Published: *May 20, 2005*

On coplanarity of most energetic cores in gamma-ray–hadron families and hadron interactions at $\sqrt{s} \gtrsim 4$ TeV

Rauf A. Mukhamedshin*

Institute for Nuclear Research, Russian Academy of Science
Prospekt 60-letiya Oktyabrya 7a, Moscow, 117312 Russia
E-mail: muhamed@sci.lebedev.ru

Abstract: The phenomenon of coplanarity of the most energetic subcores of atmospheric nuclear-electromagnetic cascades found in X-ray–emulsion chamber experiments with gamma-ray–hadron families is considered. It is shown that the phenomenon cannot be explained with cascade development fluctuations and external fields within the framework of present-day versions of quark-gluon string models as well as without assuming the manifestation of a process in hadron interactions characterized with large transverse momenta in the Lab frame of reference at energies $\sqrt{s} \gtrsim 4$ TeV.

Keywords: Gamma and Cosmic Rays.

*This work is partially supported by Russian Foundation for Basic Research, projects no. 03-02-17465 and 04-02-17083; and Ministry of Education and Science of Russian Federation, project no. LSS 1782.2003.2.

Contents

1. Introduction

The goal of this work is to attract attention of the high-energy physics community to very important experimental results indicating our lack of understanding of features of hadron interactions at super-high energies and the necessity of improving recent theories.

Investigations of superhigh-energy cosmic rays using techniques of extensive air showers (EAS) and X-ray–emulsion chambers (XREC) have formed an opinion that soft and semi-hard hadron interactions are well-described with quark-gluon string models (QGSM) [1 − 4]. On the other hand, a series of unexplained effects was observed as well. One of the most robust and transparent phenomena is the alignment of so-called energy distinguished cores (EDC) along a straight line on target planes in gamma-ray–hadron ($\gamma - h$) families (groups of high-energy ($E \gtrsim 4\,\mathrm{TeV}$) particles in EAS cores) with energies $\sum E_\gamma \gtrsim 700\,\mathrm{TeV}$ (which correspond to interaction energies of $\sqrt{s} \gtrsim 4\,\mathrm{TeV}$). This phenomenon has been first found by the *Pamir* Collaboration in XREC experiments carried out at an altitude of 4400 m a.s.l. (at a depth of 594 g$\cdot$cm^{-2} in the atmosphere) [5 − 8] and confirmed later in mountain [9] and stratospheric [10 − 12] experiments. Examples of four-core aligned families are shown in figure 1. For various reasons, the importance of this result falling beyond the framework of present-day QGSM versions remains unappreciated.

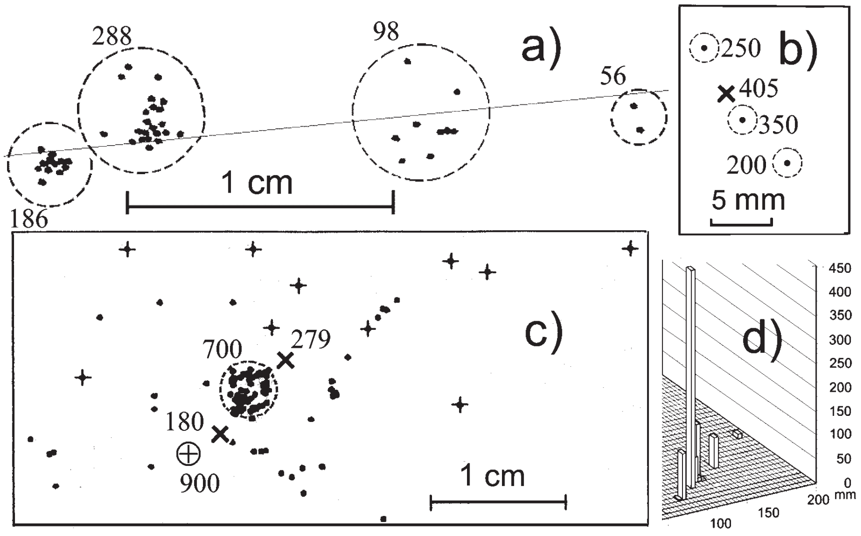

Figure 1: Examples of alignment of 4-EDC $\gamma - h$ families in XRECs. *Pamir*'s events: (a) a family composed of four aligned γ-ray clusters; (b) Pb-28; (c) Pb-6. (d) The *JF2af2* event's central part. Notation: points restricted with dotted line are clusters of γ-rays; $\times$, $+$ = hadrons, $\oplus$ = hadron halo. Parallelepiped heights and numbers mean energy in TeV.

At low $\sum E_\gamma$ values, the fraction of aligned events coincides with the background value caused by cascade development fluctuations. However, other significant deviations from the axial symmetry are observed. It is the so-called azimuthal anisotropy of particles at $\sum E_\gamma \geq 30\,\text{TeV}$ explained with models including QCD processes ([13], e.g.) and double-center ("binocular") events at $\sum E_\gamma \gtrsim 200\,\text{TeV}$ [14]. There is no a consensus of opinion on the explanation of the last phenomenon. Results of the *Pamir* Collaboration have been explained using models including QCD jets [15], whereas results [14] are not explained (in opinion of the authors of [16]) even under assumptions of preon structure of quarks.

In light of these data, the alignment does not appear as an isolated phenomenon.

Various explanations of the phenomenon were proposed, starting with a rather unsuccessful consideration of kinematic effects in diffraction processes [17 − 19]; assuming a "new" physics, namely, the appearance of a new strong interaction at energies $\sqrt{s} \gtrsim 4\,\text{TeV}$ and generation of high-p_t bosons and hadrons including super-heavy quarks of higher color symmetry [20]; exploiting processes with a high transverse momentum transfer [21, 22]; relating the effect to a projectile's diquark breaking [23]; and ending with ideas on appearance of high-spin systems [24 − 27]. As the predominant part of these ideas were proposed without accounting for development of nuclear - electromagnetic cascades (NEC) in the atmosphere, the problem has been remained unsolved.

To resolve the problem of the phenomenon interpretation, it is necessary to provide answers to the following questions.

1. Can this phenomenon be originated by cascade development fluctuations?

2. What is the physical process being capable to produce the observable phenomenon?

3. Why was this phenomenon undiscovered earlier in EAS and muon experiments?

JHEP05(2005)049

At first sight, the statistical confidence of all the experimental data seems to be not conclusive. So, it is necessary, first of all, to provide an answer to the first question with the use of a reliable algorithm for simulation of NEC development processes in the atmosphere, which is capable to describe a broad set of accelerator and XREC data. Only in the case of the negative answer, we can search with certainty for answers to remaining questions.

2. Experimental data

The *Pamir* Collaboration exploits so-called (a) "lead" and (b) "carbon" XRECs. "Lead" (Pb) XRECs consist of $60-100$ lead plates 1 cm thick sandwiched with X-ray films. "Carbon" (C) XRECs contain a 60 cm thick carbon layer placed between upper and lower parts, each of the two representing $5-6$ lead plates sandwiched with X-ray films. Cascades initiated by high-energy particles inside XRECs and producing dark spots with sizes dependent on cascade energy on X-ray films are actually detected. XRECs applied in other experiments are close to *Pamir*'s ones in principle, though they are different in design.

To analyze the alignment, the parameter $\lambda_N = \sum_{i\neq j\neq k}^{N} cos2\varphi_{ij}^{k}/[N(N-1)(N-2)]$ [5], (where φ_{ij}^{k} is the angle between vectors issuing from k-th to i-th and j-th points) decreasing from 1 (for N points disposed along a straight line) to $-1/(N-1)$ (in isotropic cases) is applied. Events are referred to as aligned, if the inequality $\lambda_N \geq \lambda_{fix}$ is valid for their N most energetic objects. Most often, $N = 4$ and $\lambda_{fix} = 0.8$.

When exploiting (a) Pb- and (b) C-XRECs, the *Pamir* Collaboration has accumulated two sets of $\gamma - h$ families; the corresponding fractions of aligned families with energies $\sum E_\gamma \geq 700\,\mathrm{TeV}$, $F(\lambda_4 \geq 0.8)$, are equal to (a) 0.43 ± 0.17 (six of the total event number $N_{fam} = 14$) [6] and (b) 0.26 ± 0.10 (9 of 35) [28], respectively. The latest C-XREC value, $F(\lambda_4 \geq 0.8) = 0.22 \pm 0.05$ (13 from 59) [29], is in a good accordance with the previous value and strengthens conclusions drawn on base of [28].

For γ-families with energy $\sum E_\gamma \geq 500\,\mathrm{TeV}$ registered in Fe-XRECs at Mt.*Kanbala* (China), the fraction of aligned events is $F(\lambda_3 \geq 0.8) = 0.5 \pm 0.2$ (3 of 6 families) [9].

Two $\gamma-h$ families with energy $\sum E_\gamma > 1000\,\mathrm{TeV}$ have been observed at high altitudes (~ 150 and ~ 10 g$\cdot$cm^{-2}, respectively), and both events are highly aligned, namely, the *Strana* ($\lambda_4 = 0.99$) [10, 11]) and *JF2af2* ($\lambda_4 = 0.998$) [12] events. In the last case, the regression coefficients of the straight line determined by the x and y coordinates of N particles, $\beta = \rho\,\sigma_y/\sigma_x$ (where ρ is the standard correlation coefficient of x and y $(-1 \leq \rho \leq 1)$; $\sigma_{x,y} = \sqrt{D_{x,y}}$), are $\beta_4 = 0.9993$ for four particles and $\beta_{38} = 0.992$ for 38 γ-rays.

A series of other important results, which fall beyond QGSM, is discussed below.

Finally, let us explain some aspects and definitions used below.

The predominant part of families is produced by primary protons with energies $E_0 \gtrsim 10\sum E\gamma$, even though their fraction in the primary cosmic radiation (PCR) is rather small. So, the contribution of nuclei is usually neglected in discussions on the alignment problem.

The term "EDC" is used in reference to the most energetic and rather isolated substructures in $\gamma - h$ families (most energetic "haloes"[1], groups of particles, and even single high-energy particles). A "decascading" procedure is used to suppress cascade multiplication processes and select EDCs by integrating particles inside subcores generated by "initial" parent particles. Starting with the most energetic (i-th, e.g.) particle, all other particles are sorted out and the parameter $z_{ik} = R_{ik}(1/E_i + 1/E_k)^{-1/2}$ (proportional to the mutual transverse momentum) is calculated. The k-th and i-th particles with energies E_i and E_k (expressed in TeV) placed R_{ik} (expressed in cm) apart are integrated, if the condition $z_{ik} < Z_c$ is fulfilled. Here Z_c is the so-called decascading parameter. Usually, at the Pamirs level $Z_c \simeq 1, 4, 20\,\mathrm{TeV{\cdot}cm}$ that correspond, on average, to the selection of particle groups originated by "initial" γ-rays, π^0-mesons, and hadrons, respectively.

It should be noted that stratospheric experiments observe the alignment of particles, while mountain experiments study the alignment of EDCs originated by these particles.

3. Simulation models

The MC0 algorithm [30] based on a QGS model [3] and broad set of accelerator data has been exploited for simulations of strong interactions of hadrons and NEC development in the atmosphere. In its features and observable results, MC0, on the whole, is closest [31–33] to the QGSJET model exploited in the CORSIKA package [34]. MC0 is the basic code of the *Pamir* Collaboration and well describes the totality of its data [35–37] at hadron interaction energies of $\sqrt{s} \lesssim 3\,\mathrm{TeV}$.

To estimate the influence of large transverse-momentum processes, a coplanar particle generation model (CPGM) was used with the following features: (a) the multiplicity is $\langle n \rangle \simeq 10$; (b) the mean transverse momentum of five most energetic particles in the coplanarity plane is $\langle p_T^{cop} \rangle = 2.34\,\mathrm{GeV/c}$; (c) the transverse momentum, normal to the coplanarity plane, is $\langle p_t \rangle = 0.4\,\mathrm{GeV/c}$; (d) the CPG interaction occurs in each of proton-initiated cascades at $E_0 \geq E_{0\,copl}^{thr} = 8$ PeV.

CPGM exploits an algorithm shown in figure 4c that is caused only by simulation usability reasons and does not result in conclusions. CPGM was only designed as a very rough heuristic tool, which reflects primitively only basic features of coplanar particle generation of the most energetic particles. CPGM does not touch, say, the problem of energy behavior of CPG cross sections, which could be described, for instance, with a logarithmic [21] or $\sqrt{s}$ [26] dependence. As the modern QGSM describes, on the whole, EAS parameters, one can expect the similarity of energetic characteristics of particles in the framework of both QGSM and a future improved CPG model.

4. Statistical fluctuations and alignment

As applied to XREC experiments, NEC development fluctuations are very strong and much more important than in EAS experiments due to a high energy particle-detection threshold ($E_{thr} \gtrsim 4\,\mathrm{TeV}$). To estimate the probability that *Pamir*'s data accumulated with the use

[1] The term "halo" is used in reference to large diffusive dark spots on X-ray films produced, as it is considered today, by well-developed atmospheric electron-photon cascades of high energy ($\gtrsim 300\,\mathrm{TeV}$).

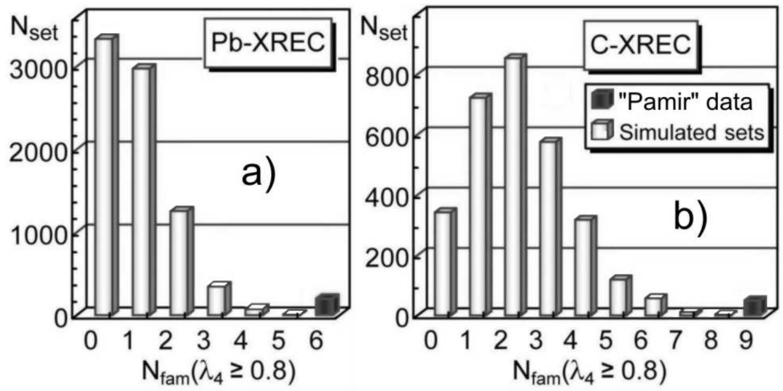

Figure 2: Distributions of number of sets of $\gamma - h$ families as functions of number of aligned events, $N_{fam}(\lambda_4 \geq 0.8)$, in each of sets consisting of (a) 14 and (b) 35 events simulated with MC0. Dark cubes denote the numbers of aligned events in the *Pamir*'s experimental family sets.

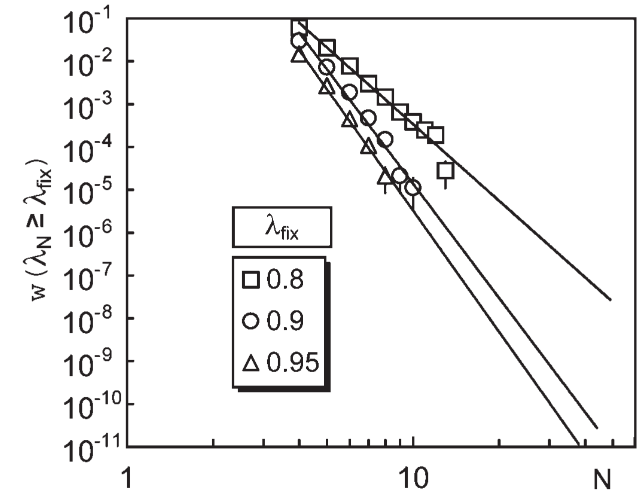

Figure 3: Dependence of $w_{fluct}(\lambda_N \geq \lambda_{fix})$ on EDC number N_{EDC} for $\lambda_{fix} = 0.8, 0.9$, and 0.95 (squares, circles, and triangles, respectively). Lines mean power-dependent fits of points.

of (a) Pb-XRECs [6] and (b) C-XRECs [28] are caused by fluctuations, (a) 8000 and (b) 3000 sets of families, respectively, have been simulated. The event number in each of these sets corresponds to experimental data. Figure 2 demonstrates the derived distributions as functions of number of aligned $\gamma - h$ families, $N_{fam}(\lambda_4 \geq 0.8)$, in each of the sets. In both the cases none of simulated sets of families coincides with the corresponding experimental set. If so, the total probability that these two statistically independent experimental results are originated by fluctuations can be roughly estimated at $\lesssim 10^{-7}$.

A more formal approach based on the binomial character of the distribution over number of aligned events has been applied as well. As is known, if the probability to satisfy some criterion is p, the probability to find k events, satisfying this criterion, among a set of n events is $P(k) = n!p^k q^{n-k}/\,[k!(n-k)!]$, where $q = 1 - p$. In our case, $n = N_{fam}$; p corresponds to the expected background fraction of aligned events, $F_{fluct}(\lambda_{3,4} \geq 0.8)$;

Data	Selection criterion	N_{exp}	$\langle N_{fluct}\rangle$	σ_{fluct}	$\Delta\sigma$	w_{fluct}
1	2	3	4	5	6	7
Pamir (Pb-XREC)	$\lambda_4 \geq 0.8$	6	1.0	1.0	5	$9 \cdot 10^{-5}$
Pamir (C-XREC)	$\lambda_4 \geq 0.8$	9	2.1	1.5	4.6	$1.5 \cdot 10^{-4}$
Mt.*Kanbala*	$\lambda_3 \geq 0.8$	3	1.2	1.2	1.5	$9 \cdot 10^{-2}$
the *Strana* event	$\lambda_4 \geq 0.99$	1	–	0.05	–	$2.9 \cdot 10^{-3}$
the *JF2af2* event	$\lambda_4 \geq 0.998$	1	–	0.015	–	$6 \cdot 10^{-4}$

Table 1: Summary of experimental and calculation data. Columns: 1. Experimental data used for the analysis; 2. Criterion for the selection of aligned events; 3. Experimental number of aligned events, N_{exp}; 4. Expected mean number of aligned events, $\langle N_{fluct}\rangle$; 5. Calculated standard deviation σ_{fluct}; 6. Deviation $\Delta\sigma$ of the experimental number from the expected value (in σ_{fluct}); 7. Probability that the experimental result is caused by fluctuations, w_{fluct}.

and $P(k)$ corresponds to the probability w_{fluct} of recording the actual value of aligned events.

While using expected background values found with MC0, namely, $F_{fluct}(\lambda_4 \geq 0.8) = 0.059 \pm 0.003$ [38] and $F_{fluct}(\lambda_3 \geq 0.8) = 0.209 \pm 0.005$, we get expected average numbers of aligned events, $\langle N_{fluct}(\lambda_{3,4} \geq 0.8)\rangle = F_{fluct}(\lambda_{3,4} \geq 0.8) \times N_{fam}$, as well as corresponding dispersions and probabilities w_{fluct} of recording the actual values for three independent sets of experimental data by the *Pamir* Collaboration and Mt.*Kanbala* experiment.

The expected background $F_{fluct}(\lambda_N \geq \lambda_{fix})$ values derived by simulations for stratospheric families [12] and [11] are equivalent in this case to observation probabilities w_{fluct}.

Table 1 presents a summary of experimental and calculation data. One can see that the maximum magnitude of the total probability W_{fluct} for the five above-mentioned statistically independent experimental results to be produced by cascade-development fluctuations is $\sim 9 \cdot 10^{-5} \times 2 \cdot 10^{-4} \times 9 \cdot 10^{-2} \times 3 \cdot 10^{-3} \times 6 \cdot 10^{-4} \simeq 3 \cdot 10^{-15}$, i.e., $W_{fluct} < 10^{-14}$.

This value calculated by using $w_{fluct}(\lambda_4 \geq 0.998)$ for the *JF2af2* event is the upper limit. Indeed, as β_N correlates strongly with λ_N at $\lambda_N \sim \beta_N \sim 1$, $N \gg 1$, and $\beta_{38} = 0.9993$, we can assume with confidence that, say, $\lambda_{38} \geq 0.95$. Figure 3 demonstrates the calculated dependence $w_{fluct}(\lambda_N \geq \lambda_{fix})$ on N for $\lambda_{fix} = 0.8$, 0.9, and 0.95. In accordance with power-dependence approximations, $w_{fluct}(\lambda_{38} \geq 0.95) \ll 10^{-9}$. If we substitute this value in place of $w_{\rm fluct}(\lambda_4 \geq 0.998)$, the total probability value decreases by more than five orders of magnitude, i.e., up to $W_{fluct} \lesssim 10^{-20}$! When taking into account that, in reality, the right tails of the distributions shown in figure 3 drop more sharply than the fit lines with increasing N, W_{fluct} must become much more less. Thus, the explanation of the alignment phenomenon with fluctuations of NEC development seems to be actually improbable.

5. Physical fields and alignment

Two natural factors are capable to influence the azimuthal features of $\gamma - h$ families, namely, the Earth's magnetic field and extreme electric fields within thunderstorm clouds.

Simulations show that the influence of the magnetic field on degree of the alignment of families cannot be actually observed at the mountain level, whereas its influence in stratospheric experiments is more efficient. However, the use of small-sized XRECs at high altitudes results in the selection of narrow events generated at small heights above XRECs. As a result, the influence of the magnetic field becomes also negligible in this case.

Under the condition that extreme electric fields with an intensity of ~ 100 kV/m and total potential of ~ 1 GV are forever in existence inside thunderclouds above XRECs, the fields could be capable to change azimuthal features of pure electromagnetic γ-families (initiated by $e^{\pm}$ or γ-rays) but not proton-initiated $\gamma - h$ families. Furthermore, thunderstorms are very rare phenomena at the Pamirs, not to mention that the maximum intensity at this height cannot exceed 50 kV/m and exponentially decreases with increasing height [39].

6. Hadron interactions and alignment

6.1 Theoretical approach

If not to mention rather unsuccessful or exotic hypotheses [17−20], other theoretical approaches to a solution of the alignment problem could be divided into two groups.

The first group exploits processes with a high transverse-momentum transfer. It is, first, a model of semihard double diffraction inelastic dissociation (SHDID) [21], which assumes the alignment to be a result of a tension of a quark - gluon string in the diffraction cluster between a semihardly scattered constituent quark and other spectator quarks of the projectile hadron and its following rupture [21] (figure 4*b*). However, the present-day version seems to be incapable for providing a sufficiently large SHDID cross section to explain experimental data. The model [22] explains the alignment as a result of generation of gluon jets that seems to be not serious as the observable alignment of the most energetic EDCs cannot be originated by low-energy gluon-jet particles.

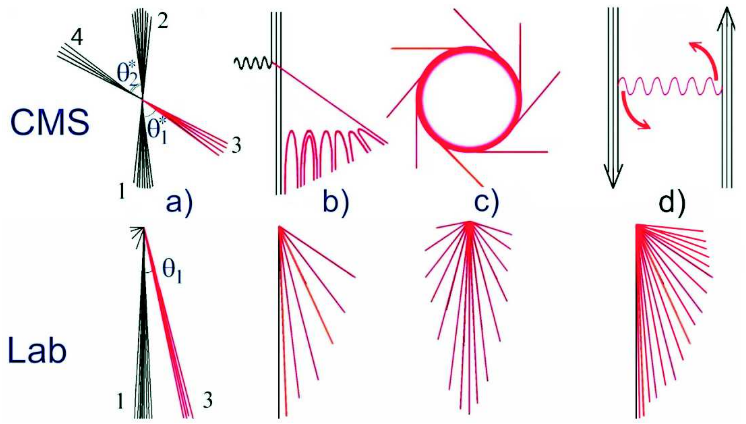

Figure 4: Types of interactions with a violation of azimuthal symmetry in CMS and Lab frames.

The second group considers origins of the appearance and coplanar decay of high-spin systems, namely, (a) the generation of heavy leading resonances [24, 25] (figure 4*c*); (b) the angular momentum conservation in the creation of a relativistic fast-rotating quark-gluon string stretched between colliding hadrons (figure 4*d*) with an angular velocity being of the order of $\omega \sim (c/b)(\sqrt{s}/M)$, where b is the impact parameter and M is the string mass [26]; (c) a consequence of relativistic properties and angular momentum conservation (with respect to the target nuclei) of semiclassical high-energy projectile hadrons [27]. The Lab-frame coplanarity of secondaries appears in [26, 27] by a natural way as a simple kinematic effect with a cross section, which could be comparable with the usual inelastic one.

Models with a high-spin rotation and coplanar decay of the noninteracting part of the projectile nucleus stand apart from these ideas. However, as the efficiency of family generation by primary nuclei is low, this idea cannot be seriously considered without assuming the cross section of interactions of the survival high-spin nuclei to be very low [40].

6.2 Qualitative results

It is phenomenologically possible to divide interactions resulting in a violation of the azimuthal symmetry of secondary particles into four classes: (a) QCD processes (figure 4*a*); (b) SHDID-like processes (figure 4*b*); (c) the formation of leading systems with a very high spin (figure 4*c*); (d) creation of a high-angular momentum quark-gluon string (figure 4*d*). Each of the classes corresponds to a certain type of (anti)correlation of particles' longitudinal and transverse momenta that results ultimately in the alignment observation probability.

When two leading jets (1 and 2) in the fragmentation range and two QCD jets (3 and 4) are generated in the center-of-mass system (CMS) of a hadron collision (figure 4*a*), XRECs observe only jets 1 and 3 in the Lab frame. If the transverse momentum of i-th particle in the jet 3 (with respect to the jet axis) is much less than both its longitudinal momentum and jet momentum, particles of jet 3 form a collimated beam in the Lab frame and a separate cluster on the target plane, i.e., create a "binocular" event (figure 4*a*). However, an alignment, as such, is not observed. On the other hand, energies of the predominant part of such jets are too small to produce observable effects with a sufficiently high probability. No doubt, this simplified representation could be incorrect, if the jet's longitudinal and transverse momenta are small, say, $P_{t\,jet} \lesssim 10\,\mathrm{GeV/c}$, i.e., if QCD is rather inapplicable.

It should be noted that the case of two QCD jets produced in CMS at $\theta_1^* \approx \theta_2^* \approx 90°$ together with the leading jet 1 could result in a triad of coplanar jets. However, the cross section of generation of jets of sufficiently high energies seems to be too low to describe experimental data. Really, it follows from simulations [41] based on the PYTHIA generator that the standard PYTHIA version provides only the background effect. A significant fraction of aligned triad events in the Lab frame could be generated only at very high interaction energies ($\sqrt{s} \sim 14\,\mathrm{TeV}$, e.g.) and very high transverse momenta of jets ($P_{t\,jet} \gtrsim 0.2\sqrt{s}$/c , i.e. at $P_{t\,jet} \gtrsim 3\,\mathrm{TeV/c}$ at LHC energies). Furthermore, there are other strong arguments against this explanation of the alignment phenomenon.

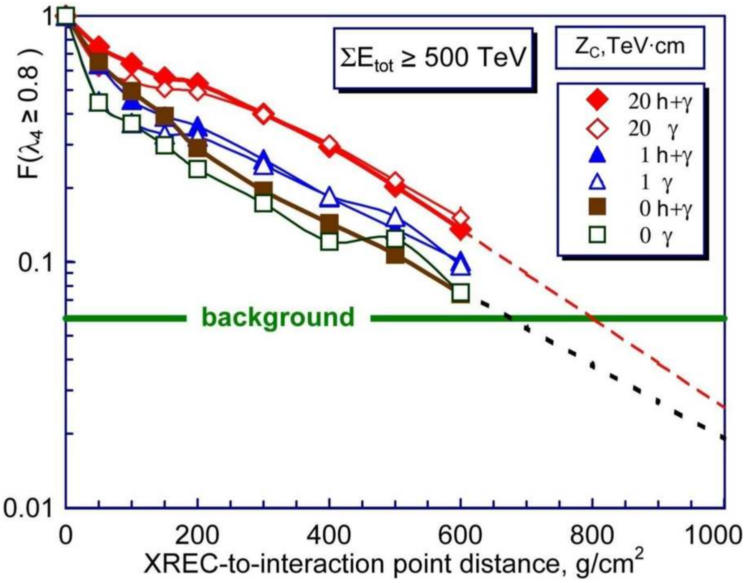

Figure 5: Dependence of $F(\lambda_4 \geq 0.8)$ on distance Δx (g$\cdot$cm^{-2}) from the CPG point to observation level at different Z_c values. Dashed lines denote extrapolations.

Within the framework of SHDID-like models assuming the alignment to be a result of the rupture of quark-gluon string stretched inside the diffraction cluster [21] (figure 4b), one could expect that the tension of the string in the cluster's CMS develops mainly back. In this model secondary particles carry a noticeable fraction of projectile particle's energy, and the alignment is observed in the Lab frame, as the required anticorrelation between $p_{t\,i}$ and $p_{L\,i}$ takes place: the larger is the transverse momenta, the lower is the energy.

The decay of high-spin hadron systems (figure 4c,d) [24−27] is characterized by a $p_{t\,i} - p_{L\,i}$ anticorrelation, favorable for the alignment observation. A detailed analysis could find differences between these models. For instance, features of secondary particles generated by a heavy high-spin leading resonance [24] (figure 4c) or by a rotating quark-gluon string stretched between colliding hadrons [26] (figure 4d), could be rather distinctive; in part, the relative (outermost or central) position of the most energetic particle is different in the Lab frame.

6.3 Analysis of experimental and simulated results

Characteristics of four most energetic EDCs in *Pamir*'s $\gamma - h$ families with energies $\sum E_\gamma \geq$ 500 TeV and events simulated with MC0 and CPGM are considered below.

Figure 5 shows the dependence of the fraction of aligned families, $F(\lambda_4 \geq 0.8)$, on distance Δx from the CPG interaction point to observation level at $Z_c = 0$, 1, and 20 TeV$\cdot$cm for all-type particles (i.e., hadrons and γ-rays) and separately for γ-rays. Horizontal line shows the background value found by MC0. Evidently, even a high coplanarity degree is quickly destroyed by cascade development processes.

Within the framework of our concept, one can conclude that (a) $F(\lambda_4 \geq 0.8)$ depends strongly on Δx; (b) $F(\lambda_4 \geq 0.8)$ depends on Z_c; (c) the CPG cross section has to be

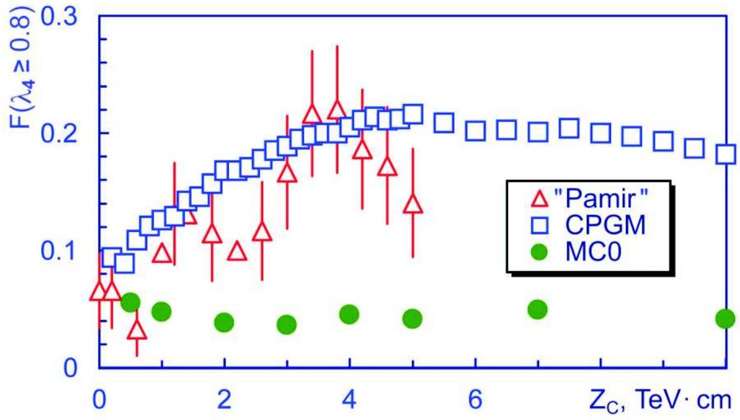

Figure 6: Dependence of $F(\lambda_4 \geq 0.8)$ on Z_c. $\triangle$– experiment [43], $\bullet$ — MC0, $\square$ — CPGM.

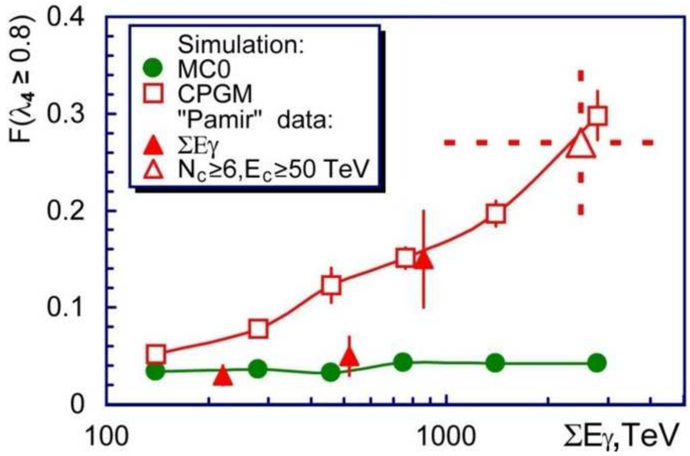

Figure 7: Energy dependence of $F(\lambda_4 \geq 0.8)$. Experiment [44]: $\blacktriangle$ — selection by $\sum E_\gamma$, $\triangle$ — selection by $N_c \geq 6, E_c \geq 50\,\text{TeV}$. Calculation: $\bullet$ — MC0, $\square$ — CPGM.

comparable with the inelastic one, $\sigma_{cop}^{p-air} \simeq \sigma_{inel}^{p-air}$, if coplanar interactions are produced by protons and $F(\lambda_4 \geq 0.8) \gtrsim 0.2$ at mountain levels.

Item (a) means that the CPG process is to be only studied in high-altitude experiments. So, it is no great surprise that the *KASCADE* Collaboration has found no effects at the sea level (~ 1000 g·cm^{-2}) [42]. Item (b) is confirmed by figure 6, which shows the dependence of $F(\lambda_4 \geq 0.8)$ on Z_c for γ-families. Both experimental [43] and simulated (CPGM) points show maxima at $Z_c \simeq 4 - 4.5\,\text{TeV}\cdot\text{cm}$.

Thus, figures 5 and 6 show the importance of using the EDC concept and suppression of cascade effects by the use of decascading procedures, as well as the dependence of efficiency of searching for alignment signs on correct choice of the observation height and Z_c value.

Figure 7 shows the $\sum E_\gamma$-dependence of $F(\lambda_4 \geq 0.8)$ for *Pamir*'s data [44], MC0, and CPGM. Apparently, experimental values rise with increasing $\sum E_\gamma$ that is described by CPGM and sharply differs from MC0 results. The right experimental point ($\triangle$) could be

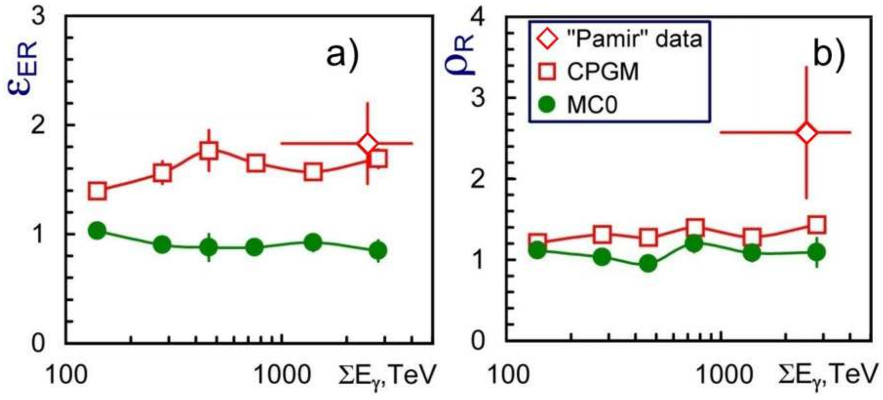

Figure 8: Dependence of (a) ε_{ER} and (b) ρ_R on $\sum E_\gamma$ for γ-families. Notations: $\diamond$ — experiment [44], $\bullet$ — MC0, $\square$ — CPGM.

slightly shifted left or right as it was found by selecting events not by $\sum E\gamma$ but by number N_c of γ-ray clusters with energy $E_c \geq 50\,\text{TeV}$ each. The same remark is valid for figure 8.

Figure 8 shows $\sum E_\gamma$-dependence of ratios of double-averaged[2] values of (a) $\langle\overline{ER}\rangle_4$ and (b) $\langle\overline{R}\rangle_4$ for aligned families to similar values of unaligned events, i.e., of variables (a) $\varepsilon_{ER} = \langle\overline{ER}\rangle_4(\lambda_4 \geq 0.8)/\langle\overline{ER}\rangle_4(\lambda_4 < 0.8)$ and (b) $\rho_R = \langle\overline{R}\rangle_4(\lambda_4 \geq 0.8)/\langle\overline{R}\rangle_4(\lambda_4 < 0.8)$. Circles and squares denote results obtained in the framework of MC0 and CPGM. Rhombuses denote values calculated using experimental data [44].

One of important evidences for the actual coplanarity existence is the different behaviour of ε_{ER} in the presence ($\varepsilon_{ER} > 1$) and absence ($\varepsilon_{ER} < 1$) of the coplanar particle generation. The same tendency occurs for ρ_R, though it is weaker than in the ε_{ER} case. On the other hand, just the experimental ρ_R value exceeds strongly even the CPGM values.

6.4 On search for alignment in muon and EAS experiments

Two causes prevented the discovery of this phenomenon earlier on. First, nobody searched for it. The *Strana* event registered about 30 years ago is analyzed only today. Secondly, traditional muon and EAS experiments are rather insensitive to this phenomenon.

Figure 9 shows the dependence of fraction $F(\lambda_{N\mu} \geq 0.6)$ of aligned groups of muons arriving at angles $\theta = 50^\circ - 60^\circ$ with energies $E_\mu \geq 1\,\text{TeV}$ on muon multiplicity N_μ simulated by the CPGM and MC0 models. For simplicity, it was assumed that muon groups fall in the center of 10-m and 100-m radius installations. One can see that even under this favorable condition, both the models give similar results. It is explained by the fact that even in the case of coplanar generation of high-energy mesons, the probability of their decay is negligible. On the other hand, the expected background alignment of muons is rather high because of influence of the Earth's magnetic field. For example, $F(\lambda_4 \geq 0.8) \simeq 0.13$ for muon groups and $F(\lambda_4 \geq 0.8) \simeq 0.06$ for $\gamma - h$ families.

[2] Double averaging of a parameter means that at first stage the averaging is made over particles of one event, after that over particles of another event, and so on. At the second stage, the found values are averaged once again (over all events).

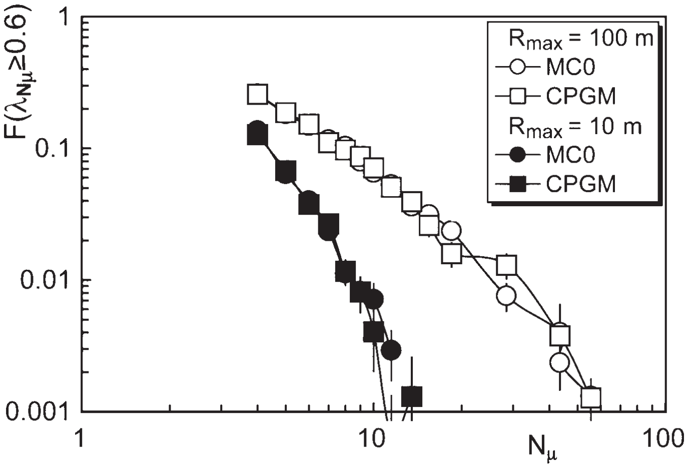

Figure 9: Dependence of the fraction of aligned muon groups, $F(\lambda_{N\mu} \geq 0.6)$, on multiplicity N_μ in the MC0 (circles) and CPGM (squares) models. Empty and filled figures correspond to 100-m and 10-m installations. $E_\mu > 1$ TeV.

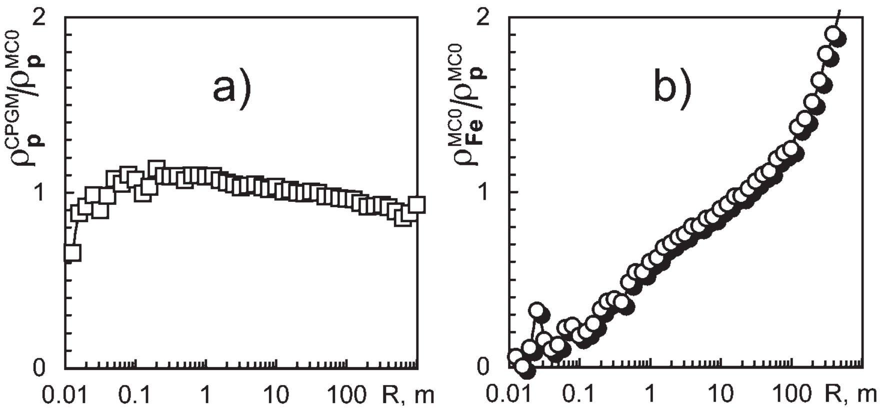

Figure 10: Dependence on distance from the EAS axis of normalized hadron densities $\rho(E_h \geq 3\,\text{GeV})$: (a) $\rho_p^{\text{CPGM}}/\rho_p^{\text{MC0}}$; (b) $\rho_{Fe}^{\text{MC0}}/\rho_p^{\text{MC0}}$. Statistical errors are not shown.

The CPG process changes EAS characteristics at a level of 700 g·cm^{-2} mainly in a narrow central range. Figure 10 demonstrates the simulated dependence of hadron densities, $\rho(E_h \geq 3\,\text{GeV})$, normalized to the proton-initiated NEC density calculated by MC0, on distance from the EAS axis: (a) the ratio of the CPGM density to the MC0 density in proton-initiated cascades; (b) the ratio of iron-initiated NEC density to that in proton-initiated cascades (both are calculated by MC0). Cascade simulations have been made at $E_0 = 5$ PeV, $E_{0\,copl}^{thr} = 5$ PeV, and $\theta = 0°$.

Figure 10a shows that the basic difference in CPGM and MC0 densities is observed in a narrow central area ($R \lesssim 0.1$ m). The difference between CPGM and MC0 at distances $R \gtrsim 1$ m is mainly caused by the difference of the models in energy spectra of secondaries. Although these results depend on CPG model, it is actually impossible to study such fine effects in EAS experiments, which, first, do not apply detectors with a high coordinate resolution and, secondly, are mainly carried out deep in the atmosphere, where the CPG influence is negligible in any case (see figure 5). Finally, figure 10b demonstrates that effects originated by heavy nuclei are much stronger, although CPG-caused effects are comparable with those produced by light nuclei and should be taken into account in EAS simulations.

6.5 On search for CPG in collider experiments

The energy dependence and other details of the coplanar particle generation could be studied at LHC by analyzing the energy deposition in $\eta \times \phi$-space cells of calorimeters of the CMS and ATLAS detectors, at energies up to $\sqrt{s} \simeq 14\,\mathrm{TeV}$, that is much higher than efficient interaction energies, $\sqrt{s_{\mathrm{eff}}^{cop}} \gtrsim 4\,\mathrm{TeV}$, corresponding to aligned events observed in XREC experiments. Certain information could be gained with CDF and D0 detectors at Fermilab; although in this case $\sqrt{s} < \sqrt{s_{\mathrm{eff}}^{cop}}$, the higher accuracy of accelerator experiments could help to discover first signs of the CPG appearance.

Scenarios shown in figure 4b,c,d are to manifest themselves by different ways. What all the scenarios have in common (and what is at once the main difficulty) is that the coplanarity is mainly related to the most energetic forward particles, which could be rather poorly studied and even inobservable at colliders at $\eta \sim \eta_{\max} \sim -\ln\{\langle p_t\rangle/[0.5\sqrt{s}(1-K_{inel})]\}$. The lower pseudorapidity-range boundary seems to be scenario dependent. When assuming for models shown in figure 4b,c that, on the one hand, the difference in energies of coplanar particles could not exceed one order of magnitude, and, on the second hand, the low-energy particles have large transverse momenta, we can estimate the lower limit as $\eta_{\min} \sim -\ln\{\langle p_T^{cop}\rangle/[0.5\sqrt{s}(1-K_{inel})/10]\}$. By assuming rather arbitrary that $\langle p_T^{cop}\rangle \sim 5\,\mathrm{GeV/c}$ and $K_{inel} \sim 0.5$, we get $\eta_{\min} \sim 2.2$ and ~ 4.2 for $\sqrt{s} \simeq 1.8$ and $14\,\mathrm{TeV}$, respectively. The first model is characterized with a rather low multiplicity of particles, while the coplanarity in the second model could be accompanied by low-energy pionization particles. The coplanarity in both these models is likely observed in one hemisphere.

The scenario shown in figure 4d is likely characterized with a higher particle multiplicity generated over all the kinematic pseudorapidity range. However, a coplanarity is to be observable in both hemispheres at higher pseudorapidity values corresponding to $p_T^{cop} > p_t$. Bounds of this range could be estimated more accurately only by exploiting a detail model of the string's rotation and fragmentation.

All these estimates are extremely rough. Improved models are required as promptly as possible to study this phenomenon both at accelerators and in cosmic-ray experiments.

7. Conclusion

Available data on the alignment of most energetic subcores of $\gamma - h$ families allow us to make the following conclusions about only the most general features of hadron interactions.

1. The alignment phenomenon can not be explained with present-day quark-gluon string models without assuming a process of coplanar particle generation with large transverse momenta manifesting itself at $\sqrt{s} \gtrsim 4\,\mathrm{TeV}$.

2. If this process occurs through interactions of protons then its cross section should be comparable with the total inelastic section at $\sqrt{s} \gtrsim 4-5\,\mathrm{TeV}$.

3. This process could be most visually described either by a hypothesis of semihard diffraction inelastic dissociation related to the pomeron physics [21] or in the framework of assumption on formation of a temporary high-spin hadron state [24 − 27].

4. This process is, most likely, similar to QGS models in energy characteristics.

5. Further investigations of the phenomenon could be carried out at LHC and Tevatron.

References

[1] A.B. Kaidalov and K.A. Ter-Martirosian, *Multiple production of hadrons at high-energies in the model of quark-gluon strings*, *Sov. J. Nucl. Phys.* **39** (1984) 979.

[2] A.B. Kaidalov, K.A. Ter-Martirosian and Y.M. Shabelski, *Inclusive spectra of secondary particles in proton nucleus interactions in the quark-gluon string model*, *Sov. J. Nucl. Phys.* **43** (1986) 822.

[3] Y.M. Shabelski, *Inclusive spectra of secondaries produced on nuclear targets at superhigh-energies and with violation of feynman scaling*, *Z. Physik* **C 38** (1988) 569.

[4] N.N. Kalmykov and S.S. Ostapchenko, *QGS model taking into account jets and EAS*, *Yad. Fiz.* **58** (1994) 21.

[5] Pamir collaboration, *Search for events with coplanar divergence of super high energy particles*, proceedings of *4th ISVHECRI*, Beijing 1986.

[6] I.P. Ivanenko et al., *Alignment in γ-hadron families of cosmic rays and characteristics of interactions at $E_0 \sim 10^{16}\, eV$*, *JETP Lett.* **50** (1992) 2125.

[7] V.V. Kopenkin, A.K. Managadze, I.V. Rakobolskaya and T.M. Roganova, *Alignment in gamma-hadron families of cosmic rays*, *Phys. Rev.* **D 52** (1995) 2766 [hep-ph/9408247].

[8] Pamir collaboration, *Alignment of cores distinguished for energies in superfamilies*, MGU-89-67-144, 1989.

[9] L. Xue et al., *Study on alignment of high energy γ-hadron family events with iron emulsion chambers*, proceedings of *26th ICRC*, Salt Lake City **1** (1999) 127.

[10] A.V. Apanasenko et al., *Stratospheric superfamily with $\sum E_\gamma \sim 2 \cdot 10^{15}\, eV$*, proceedings of *15th ICRC*, Plovdiv **7** (1977) 220.

[11] A.K. Managadze et al., *A superfamily with $\sum E_\gamma > 10^{15}\, eV$ observed in stratosphere*, proceedings of *27th ICRC*, Hamburg **1** (2001) 1426.

[12] J.N. Capdevielle, *Analysis of one cosmic ray collision near $10^7\, GeV$*, *J. Phys.* **G 14** (1988) 503.

[13] S.A. Azimov, E.G. Mulladjanov and H. Nuritdinov et al., *Azimuthal effects in hadron and photon families*, proceeding of *18th ICRC*, Bangalore **5** (1983) 458.

[14] Chacaltaya collaboration, *Gamma-ray families observed by Chacaltaya emulsion chambers*, proceeding of *17th ICRC*, Paris **11** (1981) 163.

[15] A.M. Dunaevsky, S.V. Pashkov and S.A. Slavatinsky, *Binocular gamma-families and large-p_t jets production*, proceeding of *18th ICRC*, Bangalore **5** (1983) 449.

JHEP05(2005)049

[16] Z. Cao, L.K. Ding, Q.Q. Zhu and Y.D. He, *Quark compositeness, new physics and ultrahigh-energy cosmic ray double core gamma family events*, *Phys. Rev. Lett.* **72** (1994) 1794.

[17] J.N. Capdevielle, R. Attallah and M.C. Talai, *Coplanar emission in gamma-ray families, geometrical and dynamical coincidence or new mechanism?*, proceeding of *27th ICRC*, Hamburg **1** (2001) 1410.

[18] M.D. Smirnova and Yu.A. Smorodin, *Multicore haloes and their alignment in the two-component model of hadron interactions*, proceeding of *21st ICRC*, Adelaide **8** (1990) 310.

[19] Q.-Q. Zhu et al., *Interpretation of azimuthal anisotropical gamma-family events observed by mountain emulsion chambers*, proceeding of *21st ICRC*, Adelaide **8** (1990) 306

[20] A.R. White, *Analytic multi-Regge theory and the pomeron in QCD, 2. Gauge theory analysis*, *Int. J. Mod. Phys.* **A 8** (1993) 4755 [`hep-th/9303053`].

[21] I.I. Royzen, *Theoretical approach to alignment phenomenon*, *Mod. Phys. Lett.* **A 9** (1994) 3517.

[22] F. Halzen and D.A. Morris, *Coplanar jets*, *Phys. Rev.* **D 42** (1990) 1435; *Collinear halos*, proceeding of *21st ICRC*, Adelaide **8** (1990) 18.

[23] J.N. Capdevielle et al., *Remarkable events in the knee region and abnormal behaviour in EAS data*, proceeding of *28th ICRC*, Tsukuba **1** (2003) 1599.

[24] T.S. Yuldashbaev, Kh. Nuritdinov and V.M. Chudakov, *Unusual family characteristics at energies above 10 PeV*, *Nuovo Cim.* **24C** (2001) 569.

[25] R.A. Mukhamedshin, *On a mechanism of coplanar generation of particles at superhigh energies*, *Nucl. Phys.* **75A** *(Proc. Suppl.)* (1999) 141.

[26] T. Wibig, *Alignment in hadronic interactions*, `hep-ph/0003230`.

[27] G.T. Zatsepin, private communication.

[28] A.S. Borisov et al., *Coplanar emission of high energy particles in super-families with total gamma-ray energy exceeding 400 TeV*, proceeding of *8th ISVHECRI*, Tokyo (1994) 49.

[29] A.S. Borisov et al., *Coplanar production of pions at energies above 10 PeV according to Pamir Experiment data*, proceeding of *28th ICRC*, Tsukuba **1** (2003) 85.

[30] G.F. Fedorova and R.A. Mukhamedshin, *Comparison between parameters of some models of nuclear-electromagnetic cascade simulation*, *Bull. Soc. Sci. Lettr. Lodz, Ser. Rech. Def.* **XVI** (1994) 137.

[31] H. Bielawska et al., *Characteristics of gamma-hadron families in CORSIKA and MC0 models*, proceeding of *25th ICRC*, Durban **6** (1997) 269.

[32] H. Bielawska et al., *Factorial and fractal structure of gammahadron families in CORSIKA and MC0 models*, Proc. 25th ICRC, Durban **6** (1997) 273.

[33] A.S. Borisov et al., *Characteristics of gamma families simulated by QGSJET model*, proceeding of *26th ICRC*, Salt Lake City **1** (1999) 84.

[34] J. Knapp, D. Heck and G. Schatz, *Comparison of hadronic interaction models used in air shower simulations and of their influence on shower development and observables*, Institute of Kernphysic, Forschungszentrum Karlsruhe, FZKA 5828, 1996.

[35] T.S. Yuldashbaev, Kh. Nuritdinov and A.N. Nosov, *Azimuthal correlation peculiarities in gamma families with energies* $\sum E_\gamma = 100 - 2000\, TeV$, proceeding of *26th ICRC*, Salt Lake City **1** (1999) 76.

[36] Pamir collaboration, *Testing of QGS models of hadron nucleus interactions at* $10^{13} - 10^{15}\, eV$ *on the basis of lead emulsion chamber data*, proceeding of *22nd ICRC*, Dublin **4** (1991) 113.

[37] M. Kalmakhelidze et al., *Characteristics of gamma-hadron families against chemical composition of primary cosmic rays*, Proc. 26th ICRC, Salt Lake City **1** (1999) 100.

[38] R.A. Mukhamedshin, *On question of gamma-ray — hadron family alignment and its possible origin*, proceedings of *23rd ICRC*, Calgary **4** (1993) 100.

[39] F.V. Gurevich and K.T. Zybin, *Escaping-electron disruption and electric discharges during thunderstorm*, *Usp. Fiz. Nauk.* **171** (2001) 1177.

[40] A.D. Erlykin and A.W. Wolfendale, *Novel particles or novel properties?*, *Nucl. Phys.* **75A** *(Proc. Suppl.)* (1999) 209.

[41] I.P. Lokhtin, A.K. Managadze, L.I. Sarycheva and A.M. Snigirev, *Jet activity versus alignment*, `hep-ph/0502230`.

[42] A. Iwan et al., *Investigation of geometrical structures in the hadronic shower core*, proceeding of *28th ICRC*, Tsukuba **1** (2003) 1595.

[43] A.S. Borisov et al., *Characteristics of coplanar superhigh energy events produced in nuclear interactions at* $E_0 \geq 8\, PeV$, *Nucl. Phys.* **75A** *(Proc. Suppl.)* (1999) 144.

[44] A.S. Borisov et al., *On the nature of gamma-hadron family alignment*, *Nucl. Phys.* **B97** *(Proc. Suppl.)* (2001) 118.

JHEP05(2005)049